Small Bore DI Diesel Engine Injection Rate Shaping

ABSTRACT

The impacts injection rate shaping on small bore DI diesel engines have not been extensively studied, especially under high part load conditions with high EGR rates. Testing on heavy-duty engines has already proven the benefits of injection rate shaping under high load conditions, both with and without EGR. The purpose of this study is to reveal the impact of rate shaping on a small bore DI diesel engine. The tests for this study were completed at VKA / RWTH Aachen University, using a single cylinder engine.

Achieving future NO_X regulatory limits, such as those found in US Tier2 Bin5, it is critical that NO_X is reduced particularly at the high load points in the FTP75 or US06 certification cycles. Two part load points were selected for the single cylinder tests conducted as a part of this study, because of their relevance to the certification cycles. The testing concentrated on the rectangular (Common-Rail type), ramp and boot rate shapes at high EGR rates.

Achieving the best results for emissions, efficiency and combustion noise were gained by optimizing the ramp and boot shapes in terms of angle (ramp shape) and length and height (boot shape). The rate shapes that resulted were then compared in terms of variations in the injection timing for constant EGR rates. An analysis of the data was then performed to explain the engine behavior. Zero-dimensional heat release calculations and three-dimensional CFD calculations with the open-source program KIVA 3V were used to provide the analysis. The Institute of Technical Combustion added CFD calculations, using a Representative Interactive Flamelet (RIF) model. This study developed the model calibration to the experimental results and the initial emission calculations

The ramp shape and especially the boot shape showed retardation in combustion when compared to the rectangular shape. Particularly for the boot injection shape, this leads to reduced NO_X emission and improved combustion noise for the constant start of injection and constant EGR rate, without sacrificing other emission levels or reducing engine efficiency.

INTRODUCTION

Modern DI Diesel engines have played an increasingly larger role in the passenger car market segment, due to rising global energy usage and increasing oil prices. The main reason for its growth in popularity is due to its high efficiency. In addition to turbocharging, injection systems have drastically improved. Common rail systems have entirely replaced cam-driven systems. The common rail systems provide increased flexibility for multi-injection strategies with respect to demands for modern exhaust gas after-treatment systems. However, the cam-driven injection systems did provide unique characteristics that were helpful with regards to reducing fuel consumption and emissions. The cam-driven systems provided a much higher nozzle opening and closing velocity, which reduces the seat throttling effects. Additionally, the fuel injection rate during ignition delay is less than modern common rail systems.

A combination of both the flexibility of modern common rail injectors and the benefits of cam-driven injection systems regarding reduced seat throttling effects can be found in the CoraRS Injection System. Flexible injection rate shaping with this system is enabled by forming the slope of the actuator voltage.

A number of research projects have reported the positive effect of injection rate shaping on HD DI-diesel engines under high load conditions, both with and without EGR [1], [2], [3], [4], [5], [6], [7]. However, no studies exist for injection rate shaping with small bore diesel engines operating under high load points and with respect to Tier2 Bin5 NO_X levels with very high EGR rates.

Currently, testing is being completed on a single cylinder engine using a prototype CoraRS Injection System. The goal of the study is to identify the potential reductions in emissions, increases in efficiency and reductions in combustion noise by injection rate shaping a passenger car DI diesel engine at a high part load engine operating point. The impacts of injection rate shaping on the combustion process are analyzed through CFD calculations.

SYSTEM SETUP AND REQUIREMENTS

TEST ENGINE

The single-cylinder test engine configuration is given in Table 1. The engine is boosted by an external device. The charge-air is conditioned in terms of temperature with reference to the temperature upstream the EGR supply.

Engine	
Swept Volume	~ 450 cm³
Stroke	88 mm
Bore	81 mm
Compression Ratio	16,1
Swirl (cu/ca @ max. valve lift)	1,7
Injection System	
High Pressure Pump	Bosch CP
Rail	Bosch
Injector	CoraRS
Nozzle	
Cone Angle	158°
Design	Minisac
Hydraulic Flow Rate	450 cm³ / 30 s
Hole Diameter	0,143 mm
Hole Number	7
Nozzle k-Factor	1,5

Table 1: Engine and Injection System

INJECTION SYSTEM

The injection system CoraRS is a prototype system, designed for rate shaping injections as well as multiple injections [8]. The number of injection events is not limited. A major aspect in the development of the CoraRS injector was, beside the rate shaping functionality, a fast opening of the nozzle needle in order to reduce nozzle seat throttling effects [9]. This demand was implemented by a spring loaded nozzle needle, as it is used in unit injectors. The nozzle opening speed is depicted in Figure 1 in comparison to other injection systems.

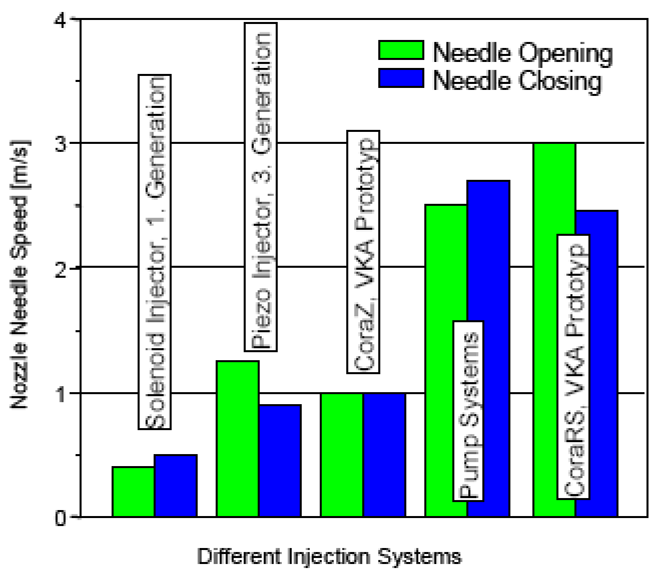

Figure 1: Nozzle Needle Speed

The injector is equipped with a needle lift sensor. Additionally, the injection pressure can be measured indirectly by tension measurement on the high pressure valve body of the injector. The tension measurement is calibrated on the injector test bench to fit the rail pressure for long injection events.

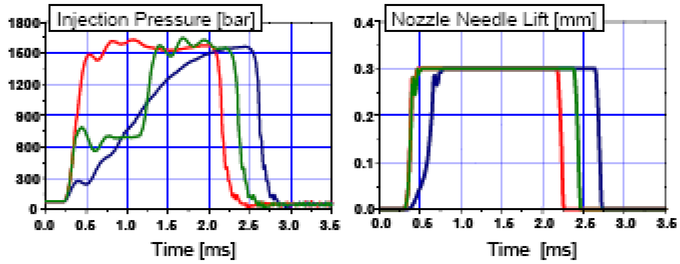

Figure 2: Rate Shapes on the Injector Test Bench

For example, possible rate shapes, measured on the injector test bench, are depicted in Figure 2. Obviously, the injection pressure is independent of the nozzle needle opening, if the injection pressure rise increases above 250 bar. The needle opening pressure is adjusted to this pressure value. The depicted ramp injection profile with its small pressure increase shows the needle opening pressure well. Of course, this ramp injection profile is not suitable for engine use and just an example of the injector's limit.

The scheme of the injector setup is displayed in Figure 3. The injection is controlled by the pre-stage valve. The pre-stage valve is charged with high pressure from the rail, which is decoupled from pressure oscillations by a dead volume and a throttle orifice. In the idle state of the pre-stage valve the high pressure circle and the control pressure are separated. The control pressure is ended to the fuel return. With the actuation of the control valve, the main valve is actuated by the pressure above the main valve piston, until balance between injection pressure and control pressure is reached. At the end of the injection, the main valve is closed by the pre-stage valve. The pressure in the injector is released by the release valve to the return line to ensure a fast nozzle needle closing.

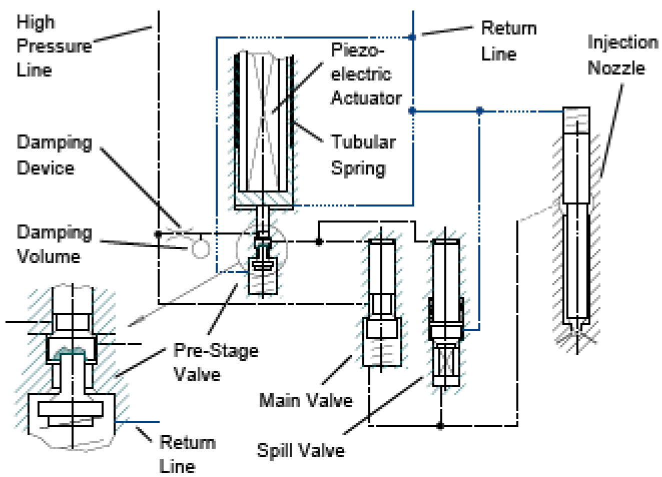

Figure 3: Scheme of CoraRS Setup

METHOD

The characteristic of rate shaping is the reduced injection rate at begin of injection (i.e. during ignition delay). To gain a constant injection quantity for different rate shapes, either the maximum injection pressure or the duration of injection have to be fitted to the quantity.

With a decreased injection rate at the beginning of injection (ramp and boot shape),

- either the maximum injection pressure (=rail pressure) has to be increased for a constant duration of injection
- or the duration of injection has to be increased while the maximum injection pressure remains constant.

This correlation is shown in Figure 4.

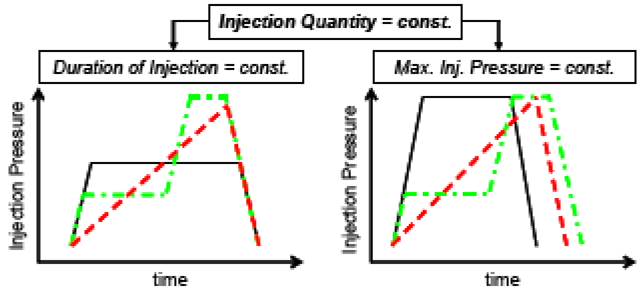

Figure 4: Measures for constant injection quantity

Both methods were tested during the experimental work.

EXPERIMENTAL RESULTS

The boundary conditions for the investigations are shown in Table 2.

No.	Speed	IMEP	PIM	PEM
-	1/min	bar	mbar	mbar
1	2280	9.4	2000	2270
2	2400	14.7	2370	2800

Table 1: Engine Boundary Conditions

OPTIMIZATION OF THE BOOT AND RAMP INJECTION SHAPE

The first part of the experimental investigation was to find a good ramp and boot injection shape. For this purpose, the angle of the ramp shape and the length and height of the boot step was varied at constant begin of injection and for a constant NOx emission.

An increased boot length results in

- drawbacks in particulate and CO emission, caused by a retarded center of combustion and
- an increase in fuel consumption, as well caused by the retarded center of combustion

The retarded center of combustion as function of the boot step length is a result of the decreased injection rate during boot step. This effect goes hand in hand with a rising duration of injection. Consequently, the boot injection with flat boot step, which generates a lower injection rate during the boot step than the medium and high boot step, indicates the highest increase in particulate and CO emission over increasing boot step length.

The effect of boot step height shows:

- Advantages in particulates and CO emission for increased boot step height and long boot step length, disadvantages concerning the same emissions for small boot step length. The influencing parameter is the ignition delay, which is strongly dependant on the boot step height.
- Disadvantages in maximum cylinder pressure rise as measure for combustion noise. The maximum cylinder pressure rise shows inverse proportionality to the ignition delay.

As an optimum boot shape, the flat boot step was chosen with a boot step length of 550 µs.

The ramp shape injection shows

- Advantages in terms of particulates, CO emission and fuel consumption for steep and medium ramp angles. Flat ramp angles lead to an increase of especially particulates and fuel consumption, which is caused by the retarded center of combustion.
- The combustion noise behaves vice versa, which corresponds to the increase of ignition delay for flat ramp angles.

The optimum ramp shape angle was chosen to 800 µs shape-length.

The injected fuel quantity was integrated for the period of ignition delay, in relation to the total fuel injected. The combination of long ignition delay and high fuel quantity during the ignition delay period results in the optimum settings, chosen above. It seems to be preferable to inject a high fuel quantity in the period of ignition delay.

The data of the zero-dimensional heat release calculation was completed as well as cylinder pressure traces and injection rates, measured at the injector test bench for the settings of the engine measurement. The measurement points are the optimum shapes, which are named above.

The difference of injection shape between the boot-step injections is comparably small due to the quite short boot step. However, the influence on the premixed combustion is clearly noticeable in the burning rate. The cylinder pressure traces show the difference as well.

The maximum injection rate of the CR-type injection is slightly higher, although the rail pressure was fixed for all injections to exactly 1400 bar. The over-boost of injection rate and thus the injection pressure can be explained by hydraulic boosting effect for a very fast opening injector. Accordingly, the ramp injection shape with a slow opening injector does not show any rate oscillations.

COMPARISON OF FLAT BOOT-STEP AND RAMP INJECTION SHAPE WITH CR-TYPE INJECTION

In the second experimental part of the investigation, the optimized settings for boot and ramp injections are compared by variation of the start of injection for constant EGR rates. The comparison is done with respect to the methods, described in Figure 4.

When keeping the duration of injection constant for variations, which affect the combustion efficiency (as for example variations of injection timing), the resulting change of the maximum injection pressure affects the interpretation of the achievement negatively. Thus, for every load point, a rail pressure was defined for each injection shape by adjusting the load for a fixed start and duration of injection and fixed EGR rate. This defined rail pressure is kept constant for the variation of injection timing, to avoid effects on the fuel-mixture generation within the variation.

The matrix of the comparison is shown in Table 3. The pilot injection in combination with the CR-type injection shape was scheduled as the state-of-the-art benchmark in terms of emission, combustion noise, and fuel efficiency. Timing and quantity of the pilot injection was optimized before.

INJECTION SHAPE	METHOD	P_{RAIL}
Boot	DOI & PRAIL const.	1400
CR-Type	DOI const.	1147
Ramp	DOI const.	1302
CR-Type with PI	DOI const.	1147
CR-Type	PRAIL const.	1400

Table 3: Matrix for Load Point 2400 rpm, 14.7 bar IMEP, Variation of Injection Timing

During the next portion of the study, three comparisons can be done:

- CR-type and flat boot-step with constant maximum injection pressure
- CR-type with and without pilot injection, ramp, and flat boot-step shape with constant duration of injection
- Influence of maximum injection pressure for CR-type injection shape in order to find the magnitude of improvements without rate shaping, just by increasing the rail pressure

The results for the comparison of CR-type and flat bootstep injection shape with the same maximum injection pressure is the following:

- The comparison of boot and CR-type injection shape for constant maximum injection pressure shows a similar particulate-NO_X trade-off with a shift to higher NO_X emission for the CR-type shape. However, the trade-off for the CR-type injection indicates slight improvements in particulate emission for a low NO_X level.
- The decrease of the maximum cylinder pressure gradient as measure for combustion noise is about factor 3 for the flat boot-step shape.
- The CO–NO_X and Efficiency–NO_X trade-off is not affected, however, the HC emission is significantly increased for the CR-type injection. This may be caused by wall wetting effects due to a higher spray penetration-depth.

The comparison of CR-type with and without pilot injection, ramp and flat boot-step shape with constant duration of injection shows that the flat boot-step shape has the best particulate-NO_X trade-off, as well the best trade-off for CO, HC and cylinder pressure rise without drawbacks in efficiency.

The CR-type injections with and without pilot injection have the worst particulate-NO_X trade-off, the CO- as well as HC-NO_X trade-off is almost the same as for ramp and flat boot-step injection.

- The flat boot-step shape shows an improvement in the combustion noise of about factor 2 in comparison with the CR-type profile w/o pilot injection. With pilot injection, the CR-type shape is comparable to the flat boot-step injection.
- The ramp injection shape shows emission- noise and fuel consumption between boot and CR-type injection profile without pilot injection.

The influence of maximum injection pressure for CR-type injection shape shall answer the question, if a simple increase of injection pressure results in similar improvements as the use of injection rate shaping.

- The improvement of the particulate–NO_X trade-off by the increase of injection pressure is significant. The CO emission and fuel consumption does not show improvements or drawbacks. However, the HC emission is increased by more than factor 2 for the high rail pressure. The combustion noise is just slightly increased.
- The advantage of the rate shaping injection, especially the boot profile, in comparison with the increase of injection pressure for the CR-type shape, is a significant reduction in combustion noise and HC emission without drawbacks in CO emission as well as fuel consumption.

The results for a constant center of combustion of 14°CA a TDC are depicted in Figure 5. The NO_X level (indicated) is about 1,4 g/kWh. This level refers to the raw emission demand for the Tier2 Bin5 legislation in this load point.

The CR-type injection with the lowest rail pressure (DOI const.) was chosen as reference for a comparison.

- For the boundary conditions of a constant duration of injection, the boot and ramp injection show benefits for particulate emission, combustion noise and slightly for CO emission. A soot reduction up to 40 % is achievable. The maximum cylinder pressure rise could be reduced for more than 30%. The CR-type injection with pilot injection can also reduce the cylinder pressure gradient (40 %) and the CO emission, but shows drawbacks in particulate emission.
- The comparison for constant maximum injection pressure (boot against CR-type) shows huge benefits for the boot injection in terms of maximum cylinder pressure gradient and HC emission.
- The increase of rail pressure for the CR-type injection without pilot injection shows a significant reduction in particulate emission (40 %) with drawbacks in maximum cylinder pressure gradient (20 %) and especially HC emission (about 200 %).

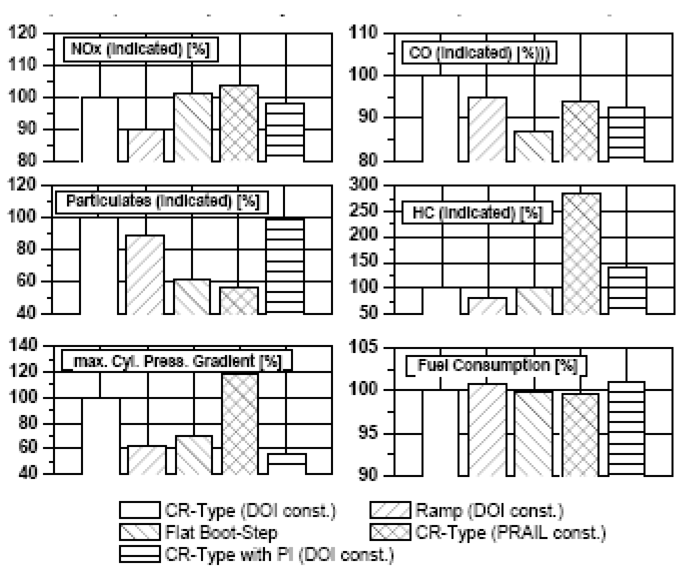

Figure 5: Center of Combustion: 14°CA aTDC at 2400 rpm, 14.7 bar IMEP

Figure 6 shows the results of the zero-dimensional heat release calculation as well as the cylinder pressure traces and the injection rate measurement from the injector test bench for the measurement points, presented in Figure 5.

The cylinder pressure traces and the traces of burned mass fraction do not show huge differences. The observed differences in emission characteristics can just be explained by the small differences in the rate of heat release in terms of the peak of premixed combustion and the maximum of heat release rate. For a deeper understanding of the correlations, especially mixture formation and turbulence, the view inside the combustion chamber is necessary. A proven method for this purpose is the CFD simulation, which delivers the thermodynamic information in a resolution of time and location in the combustion chamber. A CFD calculation, which is correlated to the measurement data, is a measure to gain additional information for understanding the processes during combustion.

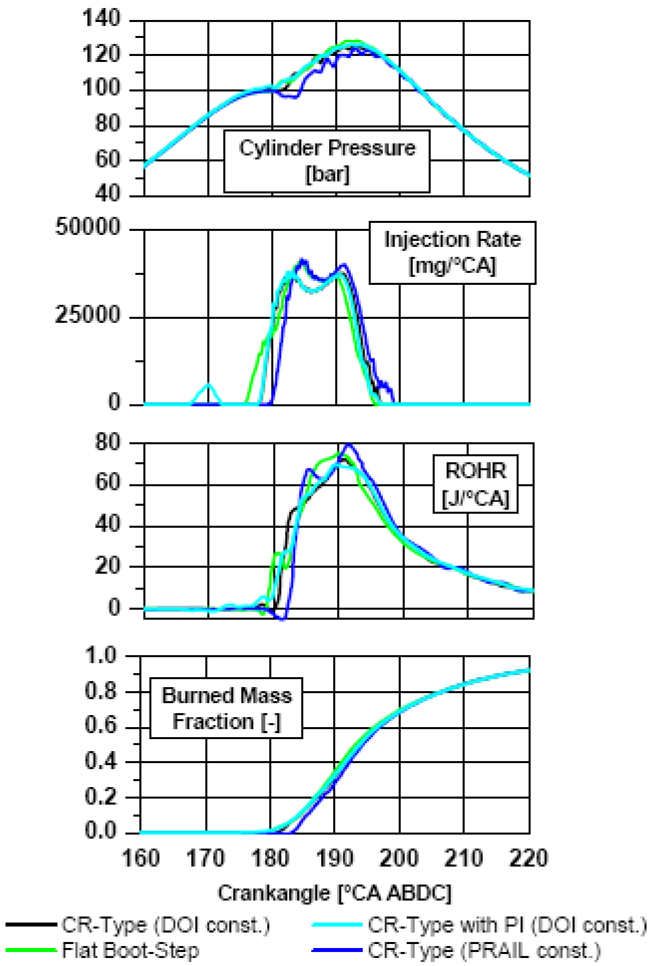

Figure 6: Variation of Injection Shapes at 2400 rpm, 14.7 bar IMEP, Center of Combustion: 14°CA aTDC, EGR-Rate: 22%

RESULTS OF CFD SIMULATION (KIVA 3V)

The simulation work was done with KIVA 3V in order to explain the observed engine behavior.

The combustion simulation model was fitted to the measured cylinder pressure traces and the rate of heat release, calculated by the zero-dimensional calculation. The fitting was done iteratively for all injection shapes. So finally one set of model parameters fitted for all injections.

The presented results are calculated for the load point 2280 rpm, 9.4 bar IMEP. The injection rates have been optimized for this load point in the same way as for the load point 2400 rpm, 14.7 bar IMEP. The engine results are depicted in Figure 7. The characteristics of the injection profiles are similar to the other load point.

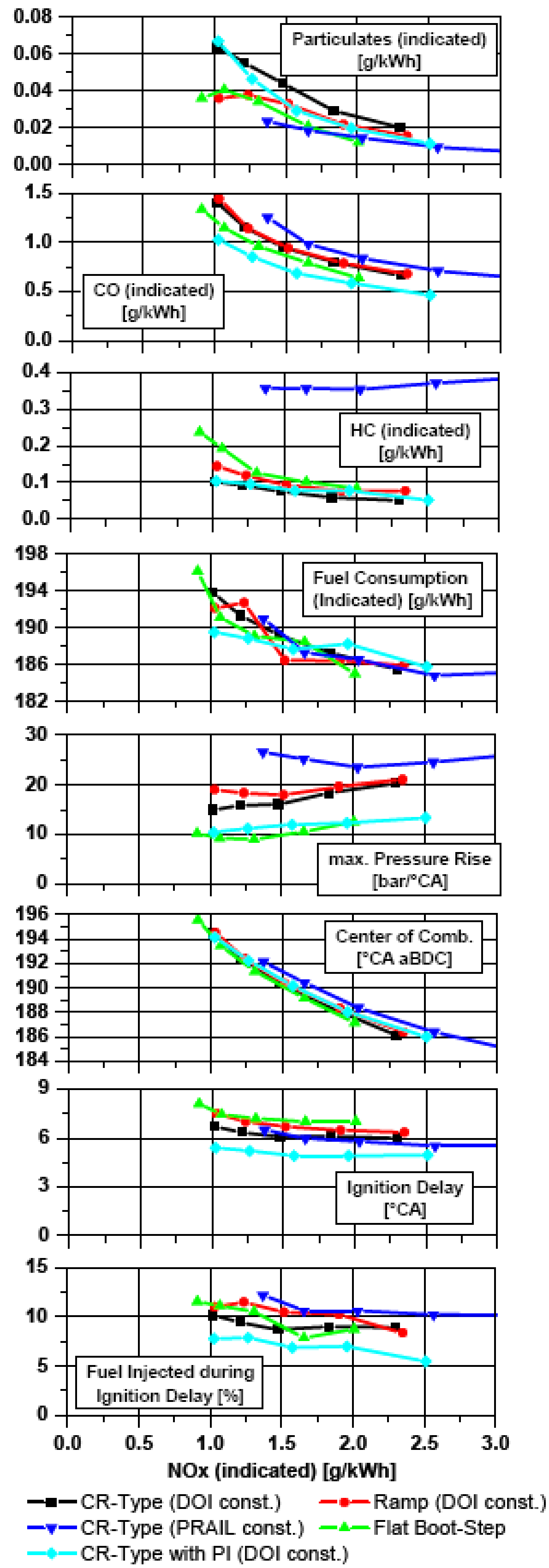

Figure 7: Variation of Injection Timing (7 to -1°CA bTDC) at 2280 rpm, 9.4 bar IMEP, EGR-Rate: 27%

The boot, ramp and CR-type injection shape (constant DOI) have been chosen for the simulation, for each shape a measurement point was selected with the earliest injection timing (greatest difference in combustion). The zero-dimensional heat release calculation is shown in Figure 8. The difference in premixed combustion is clearly noticeable in the rate of heat release, as well in the cylinder pressure rise.

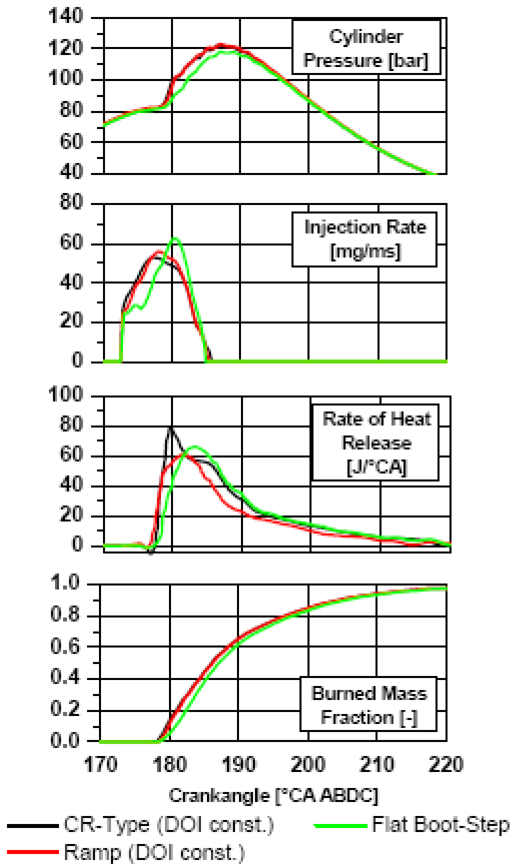

Figure 8: Variation of Injection Shape at 228rpm, 9.4 bar IMEP, SOI: 7°CA bTDC, EGR-Rate: 27%

The combustion model parameters are equal for all injection shapes, to enable a comparison of the simulation results for all injections. The emission results of the test bench and the simulation are depicted in Figure 9. The tendencies in NO_X and soot emission are met very well. The absolute differences between the injection shapes are clearly larger than the differences between measurement and simulation. The simulation results can be used for a detailed analysis of the mixture formation.

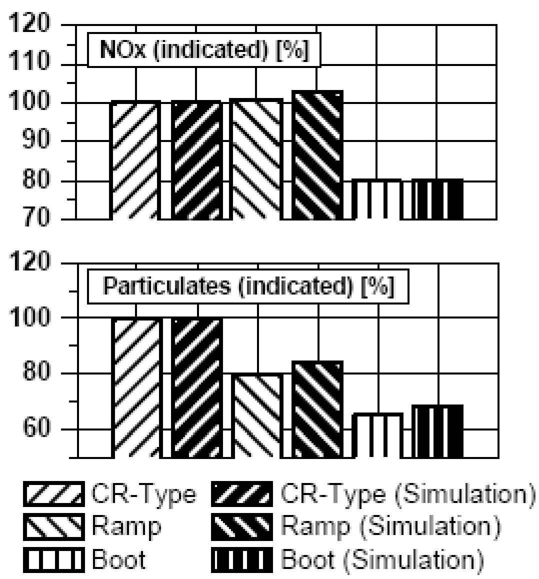

Figure 9: NOX- and Soot Emission at 2280 rpm, 9.4 bar IMEP, SOI: 7°CA bTDC, EGR: 27%

For two discrete crank angles, the results of the CFD simulation are depicted in Figure 10 and Figure 11. The boot type and CR-type (DOI const.) shape was chosen for the comparison.

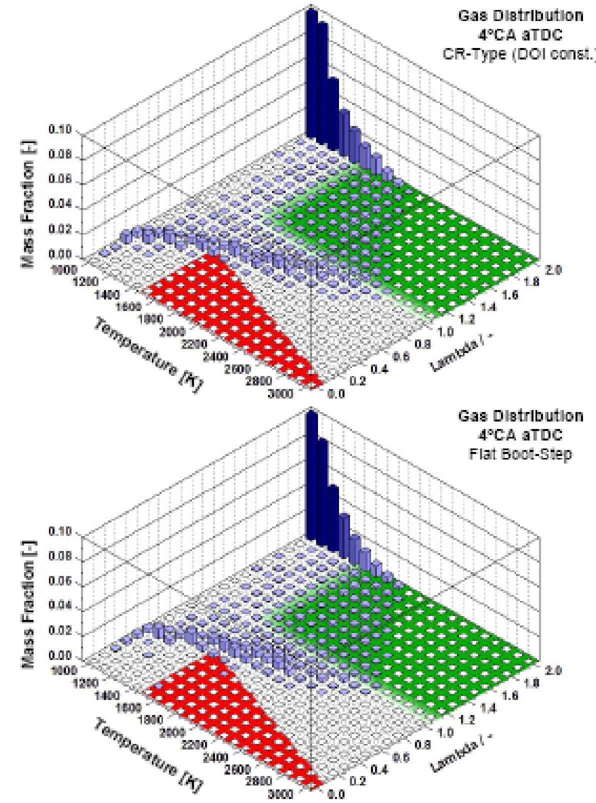

Figure 10: Gas Fraction 4°CA aTDC at 2280 rpm, 9.4 bar IMEP, SOI: 7°CA bTDC, EGR: 27%

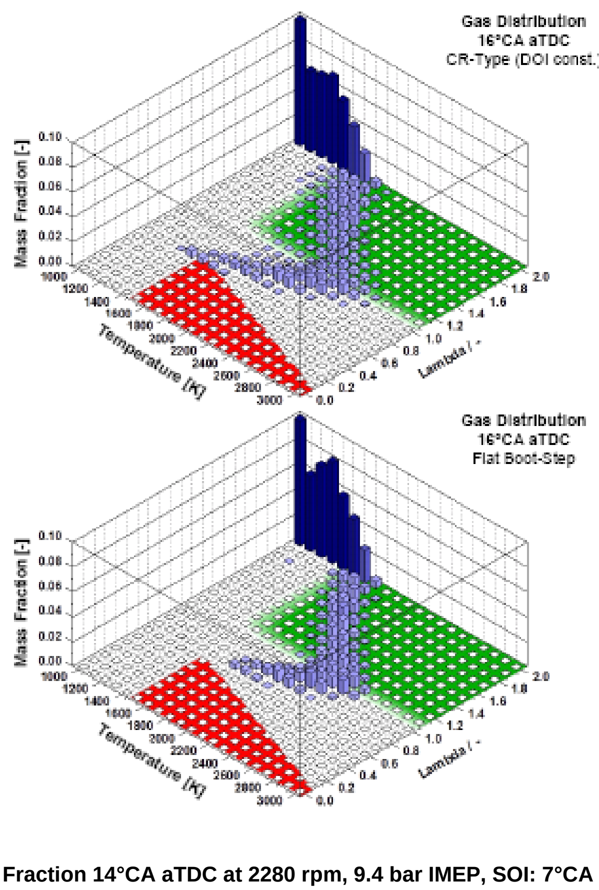

Figure 11: Gas Fraction 14°CA aTDC at 2280 rpm, 9.4 bar IMEP, SOI: 7°CA bTDC, EGR: 27%

The point of interest was the comparison of the gas distribution for certain combustion timings. The figures show the mass fraction (fuel and air) for the interesting range of lambda and temperature. In this illustration, the region of soot formation and oxidation is highlighted. The soot formation takes place at a low air-fuel ratio and low temperature. The soot oxidation proceeds in a range of high lambda and temperature. Figure 10 shows the gas distribution at the beginning of combustion. The distribution in terms of air-fuel ratio and temperature is quite similar for both injection profiles. The early phase of combustion does not show explanations for the influence of different rate shapes.

However, the later phase of combustion at 14°CA aTDC (Figure 11) shows improvements for the boot shape. The range of soot formation is already left for the boot profile, while the rectangular injection profile still shows mass fraction in the λ-T area valid for soot formation.

Figure 12 shows the calculation results in resolution of degree crank angle for CR-type, ramp and boot injection profile. The turbulent kinetic energy influences the mixture preparation during combustion. The increased turbulent kinetic energy of the ramp and especially the boot injection points to an improved mixture formation. The calculation of kinetic energy shows a similar result for both injection profiles. The graphs below give an integration of the mass fraction, which is available under conditions of soot formation and soot oxidation in terms of air-fuel ratio and temperature. This depiction gives an impression of the local mixture and thus, allows an interpretation of the engine soot emission. The boot injection profile clearly shows the lowest amount of soot formation conditions. Additionally, the rate of mass fraction under soot oxidation conditions is higher for the boot injection profile; the CR type injection shows the worst soot oxidation conditions. This correlates with the observations from the engine emission measurement.

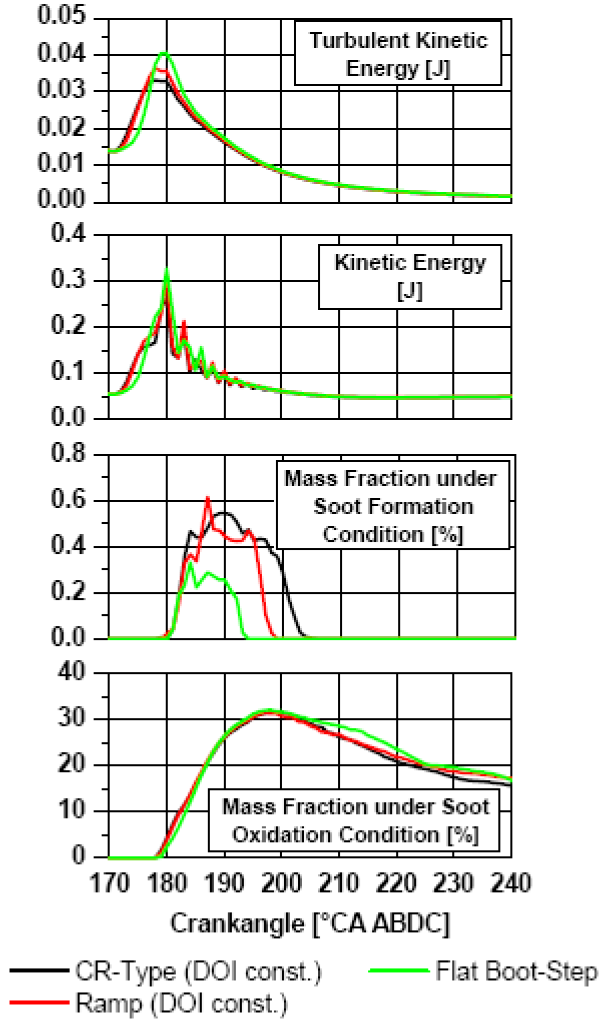

Figure 12: Summary of KIVA Results at 2280 rpm, 9.4 bar IMEP

The mixture formation in the combustion chamber is influenced by the injection rate shape. A low injection rate at the beginning of injection influences the soot formation positively by increasing the local lambda. As well, the soot oxidation is supported in the late combustion phase by the mixture formation and local temperatures.

RESULTS OF CFD SIMULATION (RIF MODEL)

The model used for three-dimensional engine simulations is based on the Representative Interactive Flamelet (RIF) for direct injection diesel engines. The RIF model effectively decouples the solution of the turbulent flow field and the diffusion flamelets. Therefore, it allows for the detailed chemistry for hydrocarbons. The CFD code solves the Navier-Stokes equations, the turbulent kinetic energy and the turbulent kinetic dissipation rate. In addition to that, the balance equations for mean and variance of mixture fraction describing the mixing field need to be solved numerically. The flamelet solution provides all scalars as a function of the mixture fraction at each time step. Mean values of these scalars are then obtained by using the pre-assumed shape pdf (probability density function). For the present work, ACFluX (formerly known as GMTEC) was used to solve fluid dynamics. It is based on Finite Volume methods [10] that employ unstructured, mostly hexahedral meshes. AC-FluX is documented in detail by Ewald et al. [11]. The RIF model has been extensively described [12–14] and applied [15-20]. Therefore, further details on the model are not presented in this paper. Rectangular, ramp and boot injection rate shapes are analyzed at a single load point (2400 rpm, 14.7 bar IMEP). Single flamelet was used for whole computational domain. The surrogate fuel (IDEA) for diesel used for simulations is a mixture of 70% (liquid) n-decane and 30% α-methylnaphthalene. The complete chemical reaction mechanism comprises 506 elementary reactions and 118 chemical species. A sector mesh representing 1/7th of the combustion chamber is used by taking advantage of the axial symmetry of the centrally located injector equipped with a 7-hole nozzle. The computations started from intake valve closure (IVC) at -120° aTDC and ended at exhaust valve open (EVO) at +120° aTDC. Trapped mass, intake pressure and temperature and measured fuel injection rate were taken from experiments. Figure 13 shows the measured injection rates.

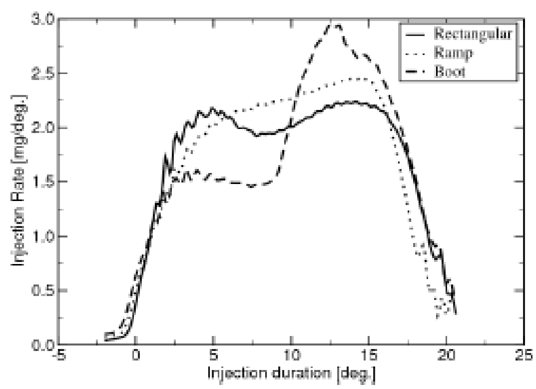

Figure 13: Injection Rate Shapes

Injection started at -1.5° aTDC and ended at 20.0° aTDC for Rectangular and Ramp injection rate shapes. While for Boot shape injection started at -2.0° aTDC and ended at 20.5° aTDC. Cylinder pressure, rate of heat release, temporal pressure gradient (signifies combustion generated noise), NOX and Soot emissions are the results of engine simulations. Figure 14 displays a comparison of measured and simulated pressure data for all the three injection rates. The figure shows an excellent overall agreement in ignition delay and peak cylinder pressure. Figure 15 display the corresponding heat release comparison. Experimental results show that the rectangular shape causes the highest premixed part in total heat release rate among the injection rate shapes which is also confirmed by the computed heat release rate. This could be attributed to that fact that higher fuel mass was injected at the beginning of injection. Injection rate shapes are well known to reduce combustion noise as shown in Figure 16. This figure confirms that a slower injection rate at the beginning of the injection leads to a smoother pressure rise.

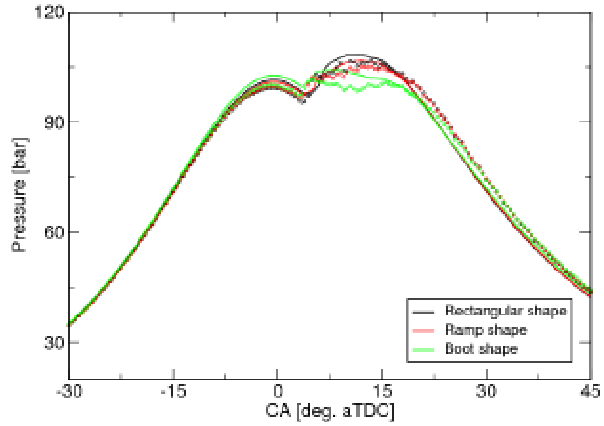

Figure 14: Measured and simulated pressure data

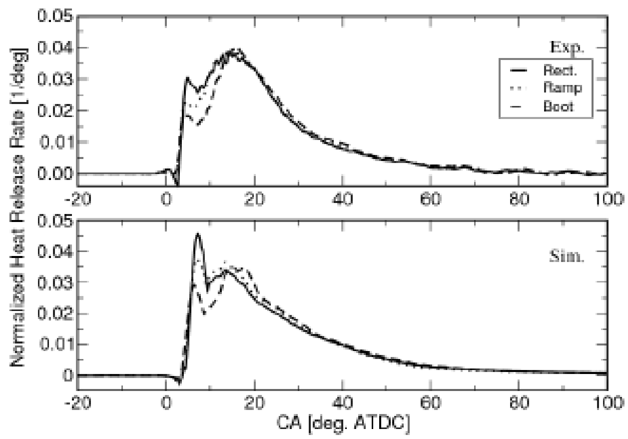

Figure 15: Heat release rates

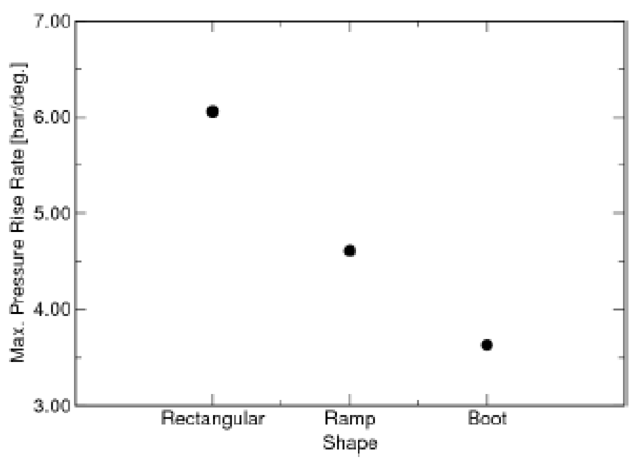

Figure 16: Maximum pressure rise rate

NO_X in physical space is computed using a PDF integration of flamelet solution for NO_X. The NO_X mechanism accounts for thermal, prompt, and nitrous oxide contribution to NO_X formation and for NO_X re-burn by hydrocarbon radicals and amines (NH_X). The result for NO_X is shown in Figure 17.

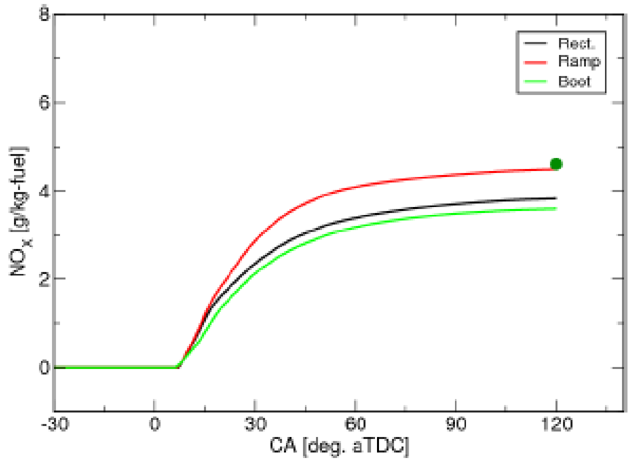

Figure 17: Comparison of NO_X emission

Although in experiments NO_X was kept constant, simulations show the deviation in results. NO_X production in engine simulations is sensitive to the in-cylinder gas temperature due to the dominance of thermal mechanism. Since constant NO_X emissions in experiments were obtained by varying the EGR levels, initial gas temperature at inlet valve closure may be different than imposed in the simulations.
The formation, the growth, and the oxidation of soot particles are described by a kinetically based model. A method using statistical moments is employed [21-22]. For the present study only the equations for the first two statistical moments are solved, which can be physically interpreted as the particle number density of soot particles and the number density of the smallest counted mass units representing the soot volume fraction. Although simulations under predict net soot (see Figure 18), nevertheless it predicts the lower soot emissions for ramp and boot shapes in comparison to rectangular shape which is in agreement with the measured soot emissions.

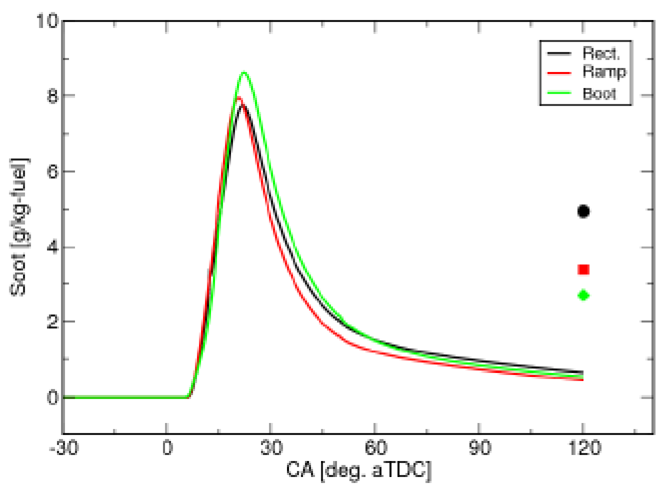

Figure 18: Comparison of soot emission

RESULTS

Combustion is influenced by rate shaping with the boundary conditions of high engine loads and high EGR rates. Engine test results have proven this with 2 load points, which are relevant for the FTP75 and US06 certification cycles.

The study compared a variety of injection shapes, such as different boot shapes, ramp shapes and a rectangular injection profile. The comparison of these injection shapes was completed with two different methods:

- The duration of injection was kept constant for all injection shapes
- The maximum injection pressure was kept constant for all injection shapes

In both cases, the boot injection shows the best characteristics, overall. The comparison for constant duration of injection points out that the boot injection shows the best emission results and the lowest combustion noise. This observation is valid for both load points. The comparison for constant maximum injection pressure shows that the effect of the boot injection shape on the engine emission is small, but results in huge improvements in combustion noise.

The evaluation of the fuel mass injected in the period of ignition delay identifies the combination of ignition delay and injected fuel amount as important parameters. The best combination was a high fuel amount injected during a long ignition delay. Only a boot injection profile with a low initial injection rate can provide these conditions.

The CFD calculations have shown that as well KIVA and AC-Flux are able to handle different injection shapes. While the analysis with AC-Flux is still ongoing, the output of the KIVA simulation shows details for the comparison of CR-type and boot injection shape for constant duration of injection. The biggest differences between both shapes are seen in the diffusion phase of combustion, where the boot profile leads to a sooner avoidance of the soot formation conditions in the combustion chamber. Additionally, the conditions for soot oxidation are improved slightly by the boot injection profile. This observation can explain the improved soot emission, measured on the test bench.

SUMMARY

The advantages of reducing combustion noise and emissions during the combustion process can be seen with a decrease in the injection rate at the beginning of injection. These injection rate characteristic advantages were created by the ignition delay and the later phase of diffusion combustion.

Beyond this study, additional boundary conditions will need to be investigated, especially the impact of injection pressure levels (2000 bar injection system) on the rate shaping effect.

OUTLOOK

This study shows the effects of injection rate shaping and injection pressure. Investigations of injections with higher injection pressure will be a part of advanced studies in the future. Injection profiles that are representative of state-of-the-art calibrations at high part load engine operation include, boot injection, CR-type with PI and eventually an additional split main injection. It is these injection profiles that will be studied in the future.

ACKNOWLEDGEMENT

The presented work was enabled by the General Motors R&D department. The authors want to thank General Motors for their kind support.

REFERENCES

1. Nishimura, Satoh, Takahashi, Yokota (Isuzu Advanced Engineering Center Ltd.): Effects of Fuel Injection Rate on Combustion and Emission in a DI Diesel Engine, SAE 981929

2. Tanabe, Kohketsu, Mori, Kawai (Mitsubishi Motors Corporation): Innovative Injection Rate Control with Next Generation Common Rail Fuel Injection System, FISITA Seoul 2000, World Automotive Congress

3. Kohketsu, Tanabe, Mori (Mitsubishi Motors Corporation): Flexibly Controlled Injection Rate Shape with Next Generation Common Rail System for Heavy Duty DI Diesel Engines, SAE 2000-01-0705

4. Kropp, Magel, Mahr, Otterbach (Bosch AG): Ein druckubersetztes Common-Rail-System mit flexibler Druckverlaufsformung, Diesel- und Benzin- DI, Einspritzsysteme - Potenziale, Anwendung, Zukunftsentwicklung, Haus der Technik Essen, 2001

5. D. Gill, F. Chmela, P. Jager (AVL List GmbH), B. Danckert (Motoren GmbH Greiner, Vogt): Emsionsund Verbrauchsverbesserungen an DI Dieselmotoren mit druckmoduliertem Common-Rail Einspritzsystem;, 11. Aachener Kolloquium Fahrzeug- und Motorentechnik 2002

6. Seebode (IAV GmbH), Delebinski, Merker (ITV, Universitat Hannover), Willmann, Teetz (MTUFriedrichshafen): Potenzialabschatzung einer freien Einspritzratenformung zur innermotorischen Emissionsreduktion an einem DI-Dieselmotor, 10. Tagung „Der Arbeitsprozess des Verbrennungsmotors“, Graz, 2005

7. Tanabe, Kohketsu, Nakayama (Mitsubishi FUSO Truck & Bus Corporation): Effect of Fuel Injection Rate Control on Reduction of Emissions and Fuel Consumption in a Heavy Duty DI Diesel Engine, SAE paper 2005-01-0907

8. H.J. Laumen, S. Pischinger, K.J. Schmucker, Th. Koerfer, M. Lamping: Flexible Einspritzverlaufsformung – auch bei PKW Dieselmotoren ein wirkungsvolles Mittel zur Reduzierung von Verbrauch und Schadstoffemissionen?

9. M. Netterscheid, H.-O. Herrmann, M. Duesterhoeft, M. Krueger: Das Potenzial von Piezo-gesteuerten Common-Rail Einspritzsystemen, Tagung Dieselund Benzindirekteinspritzung, Haus der Technik Berlin, 2000

10. J. H. Ferziger and M. Peri´c. Computational Methods for Fluid Dynamics. Springer, 3rd edition, 2002.

11. J. Ewald, F. Freikamp, G. Paczko, J. Weber, D. C. Haworth, and N. Peters. GMTEC: GMTEC Developers Manual. Technical report, Advanced Combustion GmbH, 2003.

12. N. Peters. Laminar Diffusion Flamelet Models in Non-Premixed Turbulent Combustion. Prog. Energy Combust. Sci., 10:319–339, 1984.

13. N. Peters. Laminar Flamelet Concepts in Turbulent Combustion. In Proc. Combust. Inst., volume 21, pages 1231–1250. The Combustion Institute, Pittsburgh, 1986.

14. N. Peters. Turbulent Combustion. Cambridge University Press, 2000.

15. H. Pitsch. Modellierung der Zuendung und Schadstoffbildung bei der Dieselmotorischen Verbrennung mit Hilfe eines interaktiven Flamelet-Modells. PhD thesis, RWTH Aachen, 1997.

16. H. Pitsch, Y. P. Wan, and N. Peters. Numerical Investigation of Soot Formation and Oxidation under Diesel Engine Conditions. Paper No. SAE 952357, 1995.

17. H. Barths, C. Antoni, and N. Peters. Three-Dimensional Simulation of Pollutant Formation in a DI-Diesel Engine Using Multiple Interactive Flamelets. Paper No. SAE 982459, 1998.

18. C. A. Hergart, H. Barths, and N. Peters. Modeling the Combustion in a Small-Bore Diesel Engine Using a Method Based on Representative Interactive Flamelets. Paper No. SAE 1999-01-3550, 1999.

19. C. Hasse and N. Peters. Modelling of Ignition Mechanisms and Pollutant Formation in Direct-Injection diesel Engines with Multiple Injections. Journal of Engine Research, 6:231–246, 2005.

20. V. Luckhchoura, H. W. Won, A. Sharma, G. Paczko and N. Peters. Investigation of Combustion Noise Development with Variation in Start of Injection using 3-Dimensional Simulations by Applying Representative Interactive Flamelet (RIF) Model. Paper No. SAE 2008-01-0950, 2008.

21. M. Frenklach and S. J. Harris. Aerosol Dynamics Modeling Using the Method of Moments. J. Coll. Interf. Sci., 118:252–261, 1987.

22. F. Maus. Entwicklung eines kinetischen Modells der Rusbildung mit schneller Polymerisation. PhD thesis, RWTH Aachen, 1997.